ELECTRONIC SUPPLEMENTARY INFORMATION

Force Field for Water-Surface Interaction: Is Accurate Reproduction of Experimental Water Contact Angles Enough?

Le Nhan Pham,[a] and Tiffany R. Walsh*[a]

[a]Institute for Frontier Materials, Deakin University, 75 Pigdon's Rd., Geelong, Victoria 3216, Australia

E-mail: tiffany.walsh@deakin.edu.au

Contents

1 First principles calculations

First principles methods were used to probe the potential energy hypersurfaces of adsorbates on the basal plane of MoS_2 through two steps. The first one was to benchmark density functional theory against the experimental adsorption energies, and to determine convergence of the density cutoff, kinetic cutoff of wave functions, and k-point grid. This step will assist us in identification of the most relevant density functional and parameters employed for all calculations later on. In the second step, geometrical structures of several adsorption configurations were optimized making use of the optimal cutoff, k-point mesh, and density functional. Single point (SP) calculations on all optimized configurations were carried out with a higher k-point grid and cutoff values for more reliable adsorption energies. SP energies obtained are expected to be convergent and will be used for fitting process. All quantum chemical calculations were performed with the Quantum Espresso 6.4.1 package.

In the benchmarking step, eight van der Waals-corrected density functionals (vdW-DF-c09, vdW-DF-cx, vdW-DF-ob86, vdW-DF-obk8, vdW-DF2-b86r, vdW-DF2-c09, vdW-DF, and vdW-DF2) were used to calculate adsorption energy of thiophene and butadiene on the monolayer MoS_2 basal plane. The geometrical configurations of MoS_2-adsorbate systems were optimized at the vdW-DF and vdW-DF2 levels only; energies at the other levels are single point energies using the vdW-DF geometries. The PBE projector augmented-wave (PAW) pseudopotential was utilized. Our primitive tests showed that convergence of adsorption energy (~0.07 kJ/mol) is reached when the kinetic cutoff of wave functions and charge density cutoff are 50 and 300 Ry, respectively, with a uniform k-point grid of 5x5x1. Therefore, all geometrical optimizations (described later) were conducted at this level of accuracy. More accurate energies (convergence of ~0.02 kJ/mol) were obtained with higher kinetic (75 Ry) and density (525 Ry) cutoffs, and a 7x7x1 k-point grid by performing single-point calculations. The most relevant density functional found in this step was used for all calculations in the next step.

In the second step, geometrical configurations of water on the basal plane of MoS_2 were investigated. Fifteen initial geometrical positions and directions of water were placed on the basal plane of MoS_2 and then geometrically optimized. A 4x4 supercell of MoS_2 was built from the experimental structure of the MoS_2 unit cell.[1] Since the whole substrate-adsorbate system is treated periodically in the z dimension as well, two consecutive MoS_2 layers were separated with a vacuum space of 22 Å thickness to avoid interaction between them in this direction. Fifteen water-surface configurations are given in Figure 2 of the main text and Figure S1 and of ESI.

The interaction energy (adsorption energy) was calculated using the following equation:

$$E_{ads} = E_{MoS_2+H_2O} - (E_{MoS_2} + E_{H_2O}) \quad (1)$$

where E_{ads} is the adsorption energy, and the three terms on the right-hand side are the energies of water-surface, surface, and water, respectively.

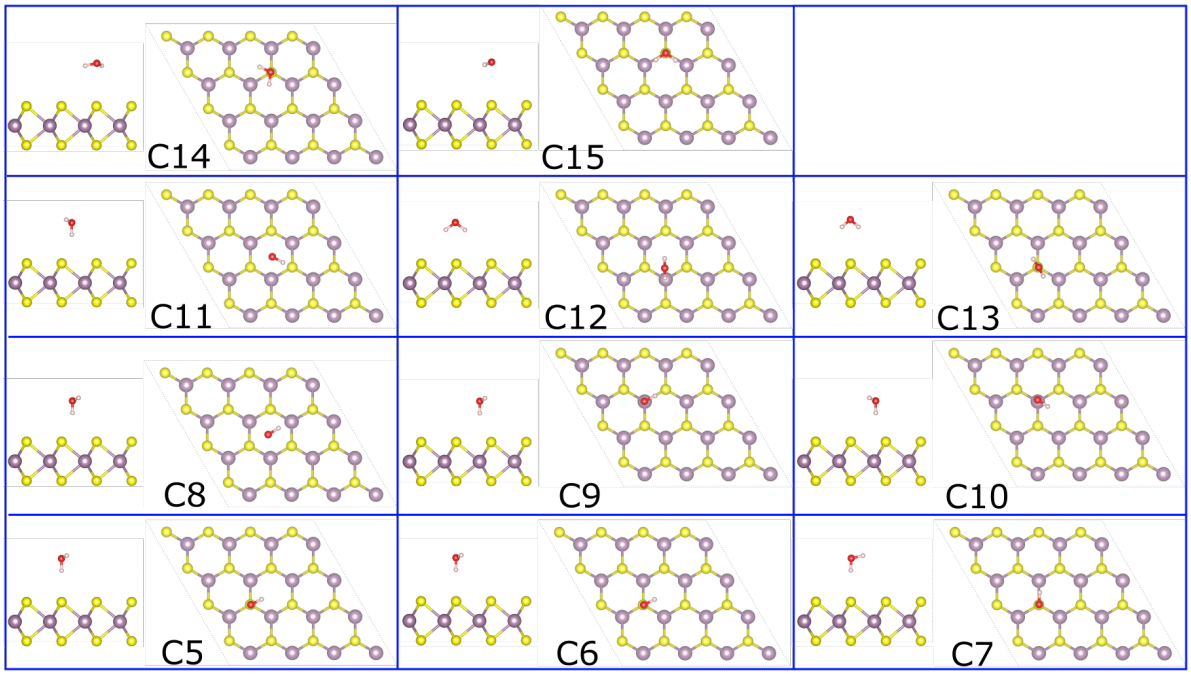

Figure S1. Side and top views of water-surface configurations determined at the vdW-DF2 level of theory

2 Force field fitting to vdW-DF2 energy

To fit the noncovalent parameters to the vdW-DF2 interaction energies of 15 geometrical configurations, a 20x20 supercell of the mono MoS_2 basal plane was created, and optimized structures of water configurations obtained from the vdW-DF2 optimizations were placed on the top of the MoS_2 surface. The vdW-DF functional tends to overshoot the distance from absorbates to surfaces; therefore, we believe that the distance from water to the MoS_2 surface should be reduced by 0.2 Å.[2,3] The whole system was treated periodically in the z direction by having multiple MoS_2 basal plans in this direction with a separation distance of 63 Å between two MoS_2 mono layers. An example of the whole system is given in Figure S2. After building the system, we calculated energy of the interaction system (E_{in}). In order to calculate the adsorption energy of water adsorbed on the MoS_2 basal plane, energy of the non-interaction system (E_{non}) (water molecule placed in the centre of the cell) was determined, and then was used as the subtrahend in Equation 2.

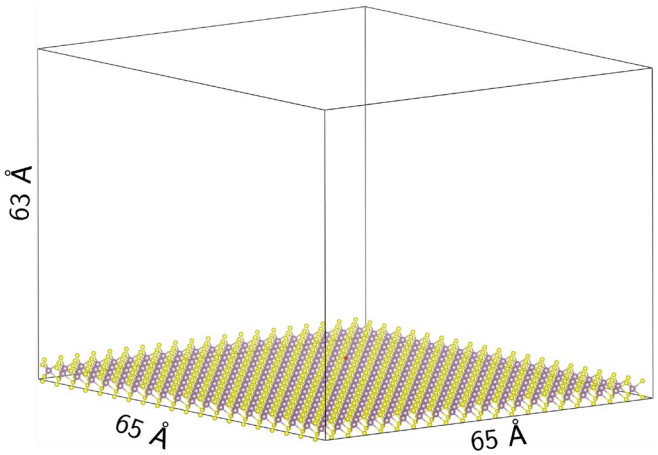

Figure S2. A 20x20 supercell used for molecular dynamics calculations during the fitting process. Dimensions of the periodic cell are provided.

$$E_{ads} = E_{in} - E_{non} \quad (2)$$

All energy calculations at this fitting step were performed making use of the Gromacs 2018.3 package. A threshold of 10 kJ/mol used to determine convergence of force. The Lennard-Jones (LJ) interactions were accounted within a distance of 11.0 Å, and smoothly turning off started from a distance of 10.0 Å. The electrostatic interactions were accounted for by using the Particle-Mesh Ewald (PME) technique with a cutoff of 11.0 Å.

The fitting process was conducted to determine the optimal parameter set. The parameter set was deemed optimal once the difference between force field and vdW-DF2 energies was as small as possible, and its energetic ranking matches that of the vdW-DF2 dataset. Note that the fitting procedure was done manually by systematically probing a whole space of parameter values. The fitting idea is that a rough and general energy hypersurface corresponding to the used space values of parameters were generated, and subsequently any energy surface wells were considered for the next refinement steps with a finer grid of values (usually up to 3 decimal digits). All good parameter values obtained from different surface wells were carefully assessed with regards to both minimization of RMSD and preserving energetic ranking. The final values of parameters should both have small (smallest) RMSD *and* the correct energetic ordering. Practically, several starting ranges of the parameter set were probed and narrowed, and in our case the range of 0 to 5 was the most suitable. All eight bespoke parameters were fitted in this range. Numerous possible combinations of non-bonded parameters were generated and narrowed through various fitting rounds by calculating energy of vdW-DF2 configurations. The parameter set that produced the small (indeed smallest) RMSD value (0.676 kJ/mol for this case) *and* the correct energetic ranking was selected as the final set.

3 Force field fitting to the experimental water contact angle

Noncovalent parameters were fitted to ensure that they can produce the experimental contact angle after extrapolation and can recover the energetic ordering of water-surface configurations determined by the vdW-DF2 functional. Three nano droplets of water with three different sizes (1500, 3000, 6000 molecules) were simulated. Contact angles of these three nano droplets were used to extrapolate the macro droplet contact angle.[4] Each droplet was formed and stabilized on the three-layer MoS_2 in a 12 ns molecular dynamics (MD) simulation in which the last 5 ns of simulations were used to calculate the contact angles. Three layers were used to simulate the bulk surface of MoS_2 in the experiment because the number of MoS_2 layers were found to influence the contact angle of water.[5] All MD simulations were conducted by using the NVT ensemble at 300K, and the temperature was maintained with the Nosé – Hoover thermostat. In order to prevent the nano droplet from interacting with its periodic images, an 80x80 supercell of three-layer MoS_2 was used for all simulations, and the vertical space between two consecutive MoS_2 substrates were set to be 204 Å. Overall, the dimensions of the simulation cell can be found in Figure S3. Note that LJ and electrostatic interactions were treated within the cutoff values mentioned above.

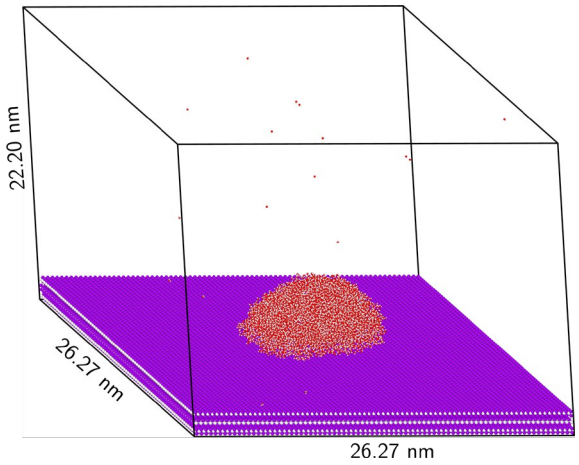

Figure S3. Dimensions of the periodic cell used for simulations of nano water droplets

To ensure that the fitted parameters can both maintain the expected droplet contact angle and recover the vdW-DF2 energetic ordering, a scaling factor was used and refined during the contact-angle fitting process. Because the droplet shape is sensitive to energy range spanned by the fitting set, and as proven in Section 5 of the ESI, the zero-point energies do contribute to the adsorption energy, and these ZPEs need to be accounted for. It is simply not practicable to calculate these ZPEs using first principles calculations for all of the configurations in the fitting set. To this end, the adsorption energies of water on the MoS_2 surface reported[6] and calculated from other five sets of published force-field parameters were used to determine a scaling factor, being 0.60. This factor was then applied to the original parameters. Note that the original parameters were obtained from the fitting process using vdW-DF2 energies without ZPE correction. A finer series (up to three decimal digits) of the scaling factor was, consequently, used for identifying the better scaling factor with an acceptable contact angle.

4 DFT benchmark results

Experimental adsorption energies of thiophene and butadiene were used to test some van der Waals density functionals as mentioned above. The most stable and low-lying geometrical configurations of these two adsorbates (T1 to T6 and B1 to B7) are given in Figure S4. Their relative energies are tabulated in Table S1. Energies calculated using three van der Waals density functionals (vdW-DF2-b86r, vdW-DF, and vdW-DF2) are in quite good correlation with the experimental values (nearly within the chemical accuracy), in which vdW-DF2 outperformed the rest. Hence, this functional was used to identify relative energetic positions of water on the pristine mono MoS_2 layer.

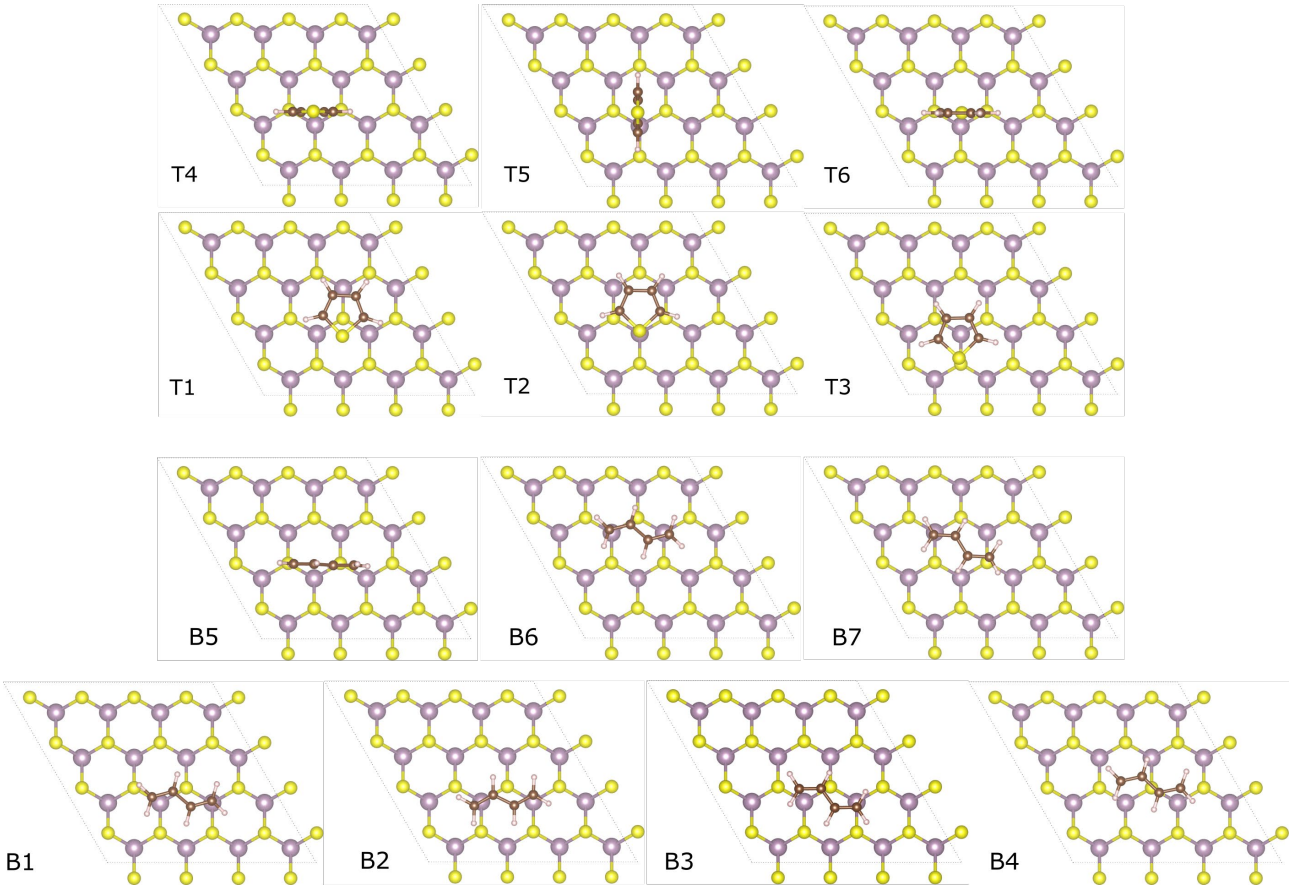

Figure S4. Geometrical configurations (top view only) of thiophene (T1 to T6) and butadiene (B1 to B7) on the mono MoS_2 basal surface.

Table S1. Adsorption energies of thiophene and butadiene on the basal plane of mono MoS_2 layer. T1 to T6 and B1 to B7 are thiophene- and butadiene-surface configurations, respectively. Experimental values are taken from refs [7] and [8].

vdW-DF	adsorption energy (kJ/mol)												
	T1	T2	T3	T4	T5	T6	B1	B2	B3	B4	B5	B6	B7
df-c09	51.71	45.72	42.60	21.66	25.97	28.10	41.91	41.75	42.26	41.58	25.28	25.28	38.77
df-cx	47.41	42.49	40.02	21.42	24.75	26.47	39.14	39.04	38.55	39.00	25.20	38.75	36.61
df-ob86	51.85	46.35	43.35	22.62	26.86	28.30	42.47	41.92	42.15	26.23	42.37	39.59	13.63
df-obk8	52.01	46.58	43.48	22.63	26.95	28.16	42.37	42.42	41.91	42.03	25.96	42.44	39.58
df2-b86r	41.60	36.20	33.27	16.11	19.79	21.43	32.59	32.55	32.03	32.21	18.57	32.54	29.80
df2-c09	33.39	28.47	28.86	11.62	14.35	28.10	25.11	25.00	24.47	24.76	13.50	24.83	22.54
df	45.24	42.15	39.98	25.81	25.81	25.46	38.35	38.69	38.11	38.12	26.30	38.28	36.75
df2	43.55	38.82	36.01	18.79	22.44	22.87	35.11	35.32	34.54	34.20	24.05	35.04	32.63
expt.	39.75							35.56					

5 Effects of zero-point energy on the adsorption energy

Three MoS_2 cluster sizes were used to investigate how ZPE affects interaction energy between water and MoS_2. Clearly, ZPE does affect the interaction energy between water and MoS_2 clusters. The proportional contribution of ZPEs to the stronger interactions (geometrical structures (a) and (b) in Figure S5) is smaller than that of ZPEs to the weaker interaction (geometrical structure (c) in Figure S5). The model (c) is quite similar to the interaction between water and the MoS_2 pristine plane used in our first principle calculations. Therefore, we believe that for the weak interaction as in the case of water adsorbed on the

MoS_2 basal plane, the proportional contribution of ZPEs is significant and subsequently impacts on the formation of the water droplet and early water contact angle.

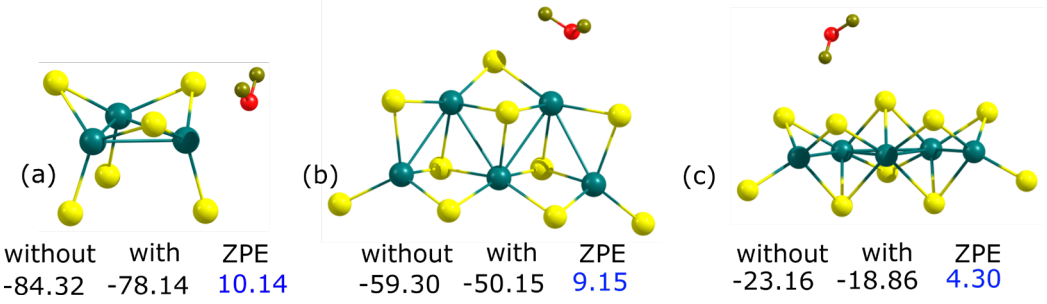

Figure S5. Interaction energies (kJ/mol) between water and MoS_2 clusters with and without correction of ZPEs.

6 Parameter sets and energetic properties

Four parameter sets SS1 to SS4 and S1 consist of the same parameters but different water models and force field families. Since these parameters were claimed to be developed for three force field families including CHARMM, AMBER, and OPLSAA, and water contact angles were tested with two models TIP3P and SPC, we used CHARMM27, AMBER99sb, and OPLSSA available in Gromacs 2018.3 to calculate the adsorption energy of 15 water-surface configurations. We can see that energies recovered by these sets behave in a similar way, quite independently of the force field families. They all identified two configurations C1 and C3 as almost non-interaction and repulsion, respectively. For the remaining sets (SS5 to SS10), because no force field families were mentioned in the publications and just the 12-6 Lennard-Jones potential was used, we used three FFs above with the reported parameters in combinations with corresponding water models reported. Again, the energetic orderings and interaction energies of water-surface configurations are almost the same among these sets (see Figure S6 and Table S4 for more details). In general, energetic orderings do not really depend on the FF families as long as they are constructed from the same noncovalent potentials.

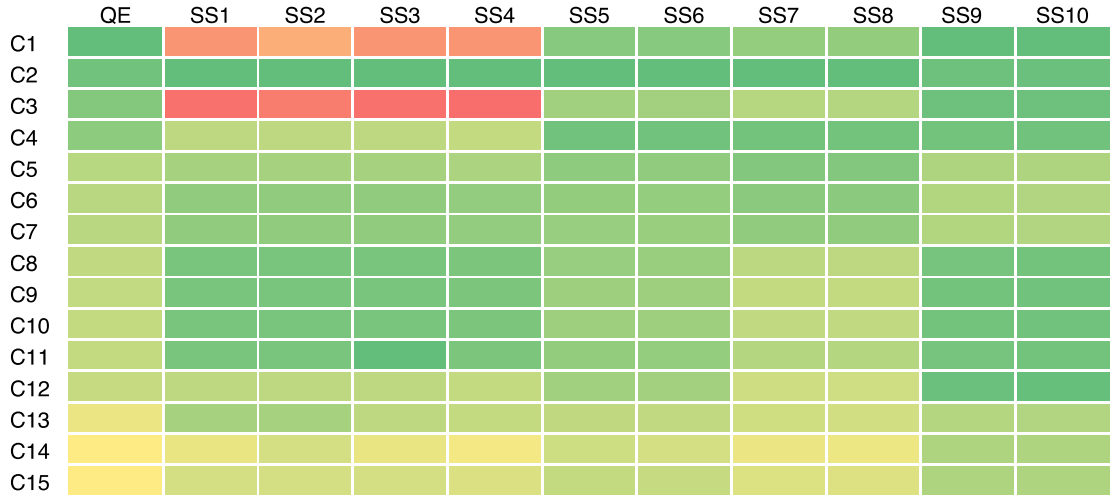

Figure S6 Energetic orderings of 15 water-surface configurations determined by 10 remaining combinations of parameter sets, water models, and force fields extracted from literature.

Table S2. Comparison of simulated contact angles produced by the five sets (S1 to S5) of force field parameters, and the experimental contact angles against which sets S1-S5 were fitting (in the

corresponding original papers). The simulation value of S4 is the work of adhesion (0.945 kcal/mol) and claimed to be close to that calculated from the experimental contact angle.

method	Contact Angle (degree)					
	S1[9]	S2[9]	S3[10]	S4[11]	S5[6]	S6[12]
simulation	69.0	69.0	69.6	0.945(*)	65.2-72.8	97.0
experiment	69.0	69.0	69.0	65-75	69.0	97.8

Table S3. Combinations of noncovalent parameters, force fields, and water models used to calculate adsorption energies given in Table S4. The AMBER99sb was used here and noted as AMBER. σ and ε are in nm and kJ/mol, respectively.

para.	para. set									
	SS1[9]	SS2[9]	SS3[9]	SS4[9]	SS5[10]	SS6[10]	SS7[11]	SS8[11]	SS9[6]	SS10[6]
σ_{Mo}	0.480	0.480	0.480	0.480	0.443	0.443	0.393	0.393	0.420	0.420
ε_{Mo}	0.293	0.293	0.293	0.293	0.485	0.485	0.192	0.192	0.254	0.254
σ_S	0.384	0.384	0.384	0.384	0.334	0.334	0.336	0.336	0.313	0.313
ε_S	1.255	1.255	1.255	1.255	2.085	2.085	1.121	1.121	1.484	1.484
q_{Mo}	+0.50	+0.50	+0.50	+0.50	+0.50	+0.50	+0.60	+0.60	+0.00	+0.00
q_S	-0.25	-0.25	-0.25	-0.25	-0.25	-0.25	-0.30	-0.30	-0.00	-0.00
FF	AMBER	OPLSSA	AMBER	OPLSSA	AMBER	OPLSSA	AMBER	OPLSSA	AMBER	OPLSSA
water	TIP3P	TIP3P	SPC	SPC	SPC/E	SPC/E	SPC/E	SPC/E	SPC/E	SPC/E

Table S4. Static adsorption energies (kJ/mol) of 15 water-surface configurations determined at the vdW-DF2 level, and calculated by using six FF parameter sets and water models reported in literature.

Config.	QE	CW	S1	S2	S3	S4	S5	S6	SS1	SS2	SS3	SS4	SS5	SS6	SS7	SS8	SS9	SS10
C1	-14.87	-7.77	-0.04	0.32	-7.91	-5.44	-6.12	-3.80	0.00	-1.00	0.00	0.00	-7.88	-7.75	-5.44	-5.44	-6.19	-6.00
C2	-14.35	-6.07	-6.82	-6.91	-8.98	-6.47	-5.97	-5.77	-7.00	-7.00	-7.00	-6.50	-8.88	-8.75	-6.47	-6.44	-6.00	-5.88
C3	-13.68	-7.77	1.64	1.81	-7.14	-4.75	-5.94	-3.09	1.50	1.00	1.50	1.50	-7.13	-7.00	-4.75	-4.75	-6.00	-5.81
C4	-13.32	-6.54	-4.76	-4.73	-8.57	-6.16	-5.87	-5.14	-5.00	-5.00	-5.00	-4.50	-8.50	-8.38	-6.16	-6.09	-5.88	-5.75
C5	-11.74	-5.38	-5.53	-5.57	-7.68	-5.84	-4.65	-5.37	-5.50	-5.50	-5.50	-5.00	-7.63	-7.50	-5.84	-5.81	-4.69	-4.56
C6	-11.70	-4.99	-6.07	-6.13	-7.55	-5.66	-4.60	-5.29	-6.00	-6.00	-6.00	-5.50	-7.50	-7.38	-5.66	-5.63	-4.63	-4.50
C7	-11.70	-4.88	-5.93	-6.00	-7.41	-5.50	-4.60	-5.09	-6.00	-6.00	-6.00	-5.50	-7.38	-7.25	-5.53	-5.50	-4.63	-4.50
C8	-11.40	-4.84	-6.47	-6.46	-7.41	-4.63	-5.79	-3.98	-6.50	-6.50	-6.50	-6.00	-7.38	-7.25	-4.63	-4.59	-5.81	-5.69
C9	-11.37	-4.78	-6.39	-6.36	-7.28	-4.47	-5.82	-3.84	-6.50	-6.50	-6.50	-6.00	-7.25	-7.13	-4.47	-4.44	-5.88	-5.75
C10	-11.31	-4.83	-6.41	-6.38	-7.31	-4.53	-5.82	-3.88	-6.50	-6.50	-6.50	-6.00	-7.25	-7.13	-4.53	-4.50	-5.88	-5.75
C11	-11.31	-4.97	-6.65	-6.59	-7.53	-4.78	-5.80	-4.22	-6.50	-6.50	-7.00	-6.00	-7.50	-7.38	-4.78	-4.75	-5.81	-5.69
C12	-11.18	-5.18	-4.85	-4.77	-7.14	-4.25	-6.03	-3.22	-5.00	-5.00	-5.00	-4.50	-7.13	-7.00	-4.25	-4.22	-6.06	-5.94
C13	-9.83	-4.23	-5.24	-5.12	-6.30	-4.22	-4.56	-3.79	-5.50	-5.50	-5.00	-4.50	-6.25	-6.13	-4.22	-4.19	-4.56	-4.50
C14	-9.06	-4.18	-4.14	-4.06	-5.88	-3.66	-4.64	-2.97	-4.00	-4.50	-4.00	-3.50	-5.88	-5.63	-3.66	-3.63	-4.69	-4.56
C15	-9.06	-4.37	-4.47	-4.39	-6.13	-3.97	-4.63	-3.34	-4.50	-4.50	-4.50	-4.00	-6.13	-6.00	-3.97	-3.94	-4.69	-4.56

References

1 B. Schönfeld, J. J. Huang and S. C. Moss, *Acta Crystallogr. Sect. B*, 1983, **39**, 404–407.
2 Z. E. Hughes, S. M. Tomásio and T. R. Walsh, *Nanoscale*, 2014, **6**, 5438–5448.
3 Z. E. Hughes, L. B. Wright and T. R. Walsh, *Langmuir*, 2013, **29**, 13217–13229.
4 T. Werder, J. H. Walther, R. L. Jaffe, T. Halicioglu and P. Koumoutsakos, *J. Phys. Chem. B*, 2003, **107**, 1345–1352.
5 Y. Guo, Z. Wang, L. Zhang, X. Shen and F. Liu, *Phys. Chem. Chem. Phys.*, 2016, **18**, 14449–14453.
6 F. Leroy, *J. Chem. Phys.*, 2016, **145**, 164705.
7 M. Salmeron, G. A. Somorjai, A. Wold, R. Chianelli and K. S. Liang, *Chem. Phys. Lett.*, 1982, **90**, 105–107.
8 S. L. Peterson and K. H. Schulz, *Langmuir*, 1996, **12**, 941–945.
9 J. Liu, J. Zeng, C. Zhu, J. Miao, Y. Huang and H. Heinz, *Chem. Sci.*, 2020, **11**, 8708–8722.
10 V. Sresht, A. Govind Rajan, E. Bordes, M. S. Strano, A. A. H. Pádua and D. Blankschtein, *J. Phys. Chem. C*, 2017, **121**, 9022–9031.
11 M. Heiranian, Y. Wu and N. R. Aluru, *J. Chem. Phys.*, 2017, **147**, 104706.
12 B. Luan and R. Zhou, *Appl. Phys. Lett.*, 2016, **108**, 131601.